The Future of Gas Turbine Technology
5th International Conference
27-28 October 2010, Brussels, Belgium

Paper ID Number: 27

CHARACTERIZATION OF A GENERIC, FUEL FLEXIBLE REHEAT COMBUSTOR

Julia Fleck, Peter Griebel, Rajesh Sadanandan, Adam M. Steinberg, Michael Stöhr, Manfred Aigner

German Aerospace Center (DLR)
Institute of Combustion Technology
Pfaffenwaldring 38-40, 70569 Stuttgart, Germany
e-mail: Julia.Fleck@DLR.de

Andrea Ciani

ALSTOM Power Ltd.
Brown-Boveri-Strasse 7, 5400 Baden, Switzerland

ABSTRACT

The development of fuel flexible gas turbine (GT) combustors is currently of a high interest in the GT industry because of the desire to employ a broader spectrum of primary energy sources. In order to investigate fuel flexibility related phenomena in the reheat combustion concept that is applied in ALSTOM®'s GT24® and GT26® family[1], a generic reheat combustor with excellent optical access has been developed. The combustor performance using different fuels at gas turbine relevant conditions ($p = 15$ bar, $T > 1000$ K, relevant gas composition) was studied with classical measuring techniques and laser diagnostics. The conditions in the mixing zone of the reheat combustor first were investigated in terms of the temperature homogeneity, velocity field, and gas composition in order to provide well-defined boundary conditions for subsequent studies of unwanted autoignition. In addition, the overall performance of the reheat combustor was measured.

The onset of unwanted autoignition in the mixing section was studied using high-speed luminosity measurements. The combustor could be operated with natural gas (NG), including "off-spec" NG containing high amounts of higher hydrocarbons (up to 25 vol. % propane), without autoignition occurring in the mixing zone. In contrast, autoignition immediately occurred in the mixing zone when injecting a hydrogen/nitrogen blend of 80/20 by volume.

Keywords: fuel flexibility, reheat combustion concept, autoignition, laser diagnostics

INTRODUCTION

Increasing interest in low-carbon fuels has led to the emergence of a broad range of primary energy sources for stationary gas turbines (GT). Besides natural gas of different qualities, the use of H_2-rich fuels from coal or biomass gasification may be an option (Campbell et al., 2008). Future stationary gas turbines therefore must be increasingly fuel flexible and able to operate with highly-reactive fuels. This poses special challenges to achieving safe, reliable, and low-emission GT combustor performance. At the same time GTs need to meet extremely strict emission targets, which are nowadays achieved with lean premixed combustion (LPC) systems. Operating such systems with highly reactive fuels significantly affects combustion properties like flame stability, flashback, and autoignition (e.g. Lieuwen et al., 2008).

One particular lean premix combustion concept is the sequential, or reheat combustion system shown in Figure 1, which is used in ALSTOM®'s GT24® and GT26® family of engines (Güthe et al., 2009; Joos et al., 1996). This concept is characterized by two separate combustion chambers with an exhaust gas expansion step in a high-pressure turbine stage in between. The operating conditions in the mixing zone of the second combustor (reheat combustor) are very different from those of

[1] ALSTOM® is a registered trademark; GT24®, GT26® are registered trademarks of ALSTOM Technology Ltd.

classical LPC systems in terms of temperature and gas composition. In a reheat combustor, secondary fuel is injected into a mixing zone containing exhaust gas at a high temperature (above 1000 K), leading to tightened flashback margins and extremely short ignition delay times. To avoid autoignition in the mixing zone, the residence time of the non-homogeneous fuel/exhaust gas mixture must be lower than the ignition delay time. Proper design of the mixing section therefore requires detailed knowledge of the ignition delay time for the fuels of interest at the relevant operating conditions, along with the flow and temperature conditions in the mixing zone.

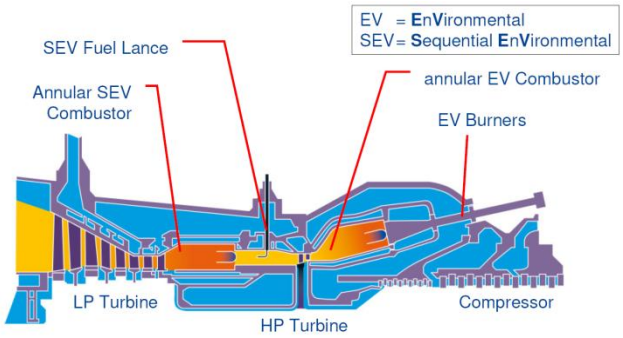

Figure 1: Sequential combustion system of ALSTOM®'s GT24® and GT26®. EV® is first stage combustor, SEV® is second stage 'reheat' combustor[2].

The ignition delay time, τ_{ign}, is defined as the time between the formation of a reactive mixture and the onset of chemical reactions leading to a rapid rise in temperature and radical concentration. Such localized autoignition events depend on the pressure, temperature, and gas composition, and can initiate large-scale ignition and combustion processes. Ignition delay times measured at well defined conditions, e.g. in shock tubes or rapid compression machines, are mainly controlled by chemical kinetics. The kinetic parameters influencing the ignition delay can be studied at these well defined conditions. Such results provide a database that is used to validate reaction mechanisms, e. g. (Herzler and Naumann, 2009). In technical combustion systems, the ignition delay additionally is influenced by physical factors like turbulent mixing and diffusion, which affect the local stoichiometry and mixture temperature because of different fuel and oxidizer temperatures. Hence, these physical factors have to be considered when investigating ignition delay times relevant for technical systems. Additionally, the exhaust gas composition entering the mixing zone of a reheat combustor must be considered since it also influences the ignition delay time (Lee et al., 2009; Riccius et al., 2005).

[2] EV®, SEV® are registered trademarks of ALSTOM Technology Ltd.

Shock tube studies of methane-based fuels (CH_4 with C_2H_6, C_3H_8, C_4H_{10}, C_5H_{12} or H_2) at reheat combustor relevant pressures and temperatures were summarized by De Vries and Petersen (2007). Higher hydrocarbons such as ethane or propane were found to reduce the ignition delay compared to pure methane/air mixtures (Koch et al., 2005; Huang and Bushe, 2006). According to Huang and Bushe (2006) this effect is due to an enhanced formation of OH radicals and is more apparent at temperatures below 1100 K. The impact of higher hydrocarbons at reheat conditions was investigated by Riccius at al. (2005). It was concluded that the ALSTOM® engines are capable of operating using NG with higher hydrocarbon contents up to 16 vol. % without requiring any hardware changes.

For hydrogen, Mittal et al. (2006) provide a literature overview indicating that only a few shock tube investigations have been carried out at pressures and temperatures relevant for the reheat system. In a recent study, Herzler and Naumann (2009) investigated pure hydrogen, a methane blend (92 vol. % methane, 8 vol. % ethane), and mixtures of both fuels in Oxygen/Argon at temperatures between 900 and 1400 K, pressures of 1, 4 and 16 bar, and two different equivalence ratios of Φ= 0.5 and 1.0. At the highest pressure of 16 bar, the ignition delay of hydrogen showed almost no dependence on the equivalence ratio, in contrast to the methane based blend. Further, τ_{ign} decreased with increasing hydrogen content, which also is reported in (Petersen et al., 2007), and (Lieuwen et al., 2008). According to Lieuwen et al. (2008), this effect is more distinct at higher temperatures. Contrary to NG/higher hydrocarbon blends, no systematic investigations on hydrogen-rich fuels at reheat conditions - namely appropriate pressure and temperature levels, fuel being injected into exhaust gas instead of air, and relevant physical processes such as premixing of fuel and exhaust gas - have been carried out in the past.

This paper characterizes the mixing section of an optically accessible, generic reheat combustor in terms of gas composition, temperature, and velocity field. Classical measuring techniques and laser diagnostics were used to measure the mixing zone boundary conditions, which are key for autoignition studies. Natural gas tests were used as a benchmark and provided a link to the practical combustion system. For NG as well as NG + 25 vol. % propane, the reheat combustor showed reliable performance. In addition, studies of unwanted autoignition in the mixing section with a H_2/N_2 blend are described.

EXPERIMENTAL SETUP

Reheat combustor

The reheat combustor schematically illustrated in Figure 2 is composed of three main sections. The first section is the so-called hot gas generator (HG), which

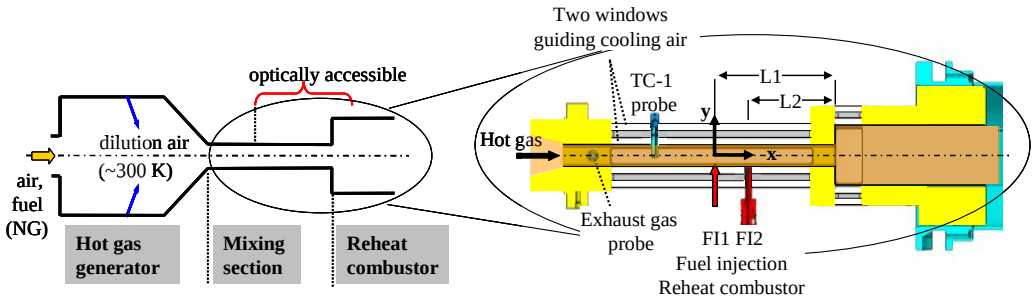

Figure 2: Sketch of generic, reheat combustor

generates hot gas of a temperature and composition representing the exhaust gas after the high-pressure turbine stage in the technical system. In a subsequent mixing section (MS), fuel is injected into the hot gas. A flame stabilizes in the reheat combustion chamber further downstream.

A slightly modified FLOX® burner (Lückerath et al., 2008) with extensive internal exhaust gas recirculation is used in the hot gas generator. It is operated solely with NG and air that is preheated to temperatures of 673 - 910 K, at equivalence ratios between Φ_{HG} = 0.4 - 0.47, and at a maximum thermal power of 420 kW. The typical NG quality used in this study is listed in Table 1 (Wobbe Index 53 MJ/m^3 @ 273 K (calculated according to Lechner and Seume, 2003)). The HG exhaust gas is mixed with dilution air before entering the MS in order to obtain hot gas at a temperatures and oxygen concentrations that are representative of the practical engine.

Table 1: Natural gas composition [volume %]

CH_4	C_2H_6	C_3H_8	C_4H_{10}	N_2	CO_2
94.2 - 98.7	3.3 - 0.8	0.9 - 0.2	0.2 - 0.1	1.3 - 0.4	0.1 - 0.3

The MS is composed of a 25 x 25 mm square duct equipped with large quartz glass windows on each side. When assembled into the employed high-pressure test rig, the field of view in the MS ranges in x-direction from approximately 3 mm downstream of FI_1 (see Figure 2) to 26 mm upstream of the cross-sectional jump at the entrance of the reheat combustor, and ± 9 mm in the y-direction. The reheat combustor fuel is injected as a jet-in-crossflow from the lower wall, representing one single injection point of a multiple point fuel injector that typically is used in gas turbine combustors. The fuel injector can be mounted at either of the two axial positions FI_1 or FI_2, thereby changing the mixing length (L_1 to L_2) and the residence time of the fuel/hot gas mixture in the MS by a factor of 1.5. To keep the fuel jet penetration about the same, a fuel injector diameter (d_{fi}) of 2.4 mm is used for NG and 5.6 mm for the H_2/N_2 blend.

The reheat combustor geometry is characterized by a cross-sectional jump to 70 x 70 mm. The reactive mixture autoignites at the combustor inlet and a flame stabilizes in the reheat combustor due to the outer recirculation zones. Quartz glass windows (30 x 64 mm, length x height) in all four reheat combustor walls provide optical access to the flame root region.

Air- and water cooling systems are used to cool the combustor walls and are designed to operate with minimal heat loss. In the MS only the metal parts that are coated with a zirconium-oxide thermal barrier coating (TBC) are water cooled, resulting in a relatively low overall heat loss of about 6%. The heat loss was calculated by taking into account the enthalpy increase of the cooling air and cooling water between the in- and outflows and the thermal power of the combustor. The reheat combustion chamber also is TBC coated and partly water cooled.

Integrated in the high-pressure combustion test rig in Stuttgart (HBK-S), large windows allow the use of laser diagnostics in the mixing section and reheat combustor. A detailed description of the test rig can be found in (Fleck et al., 2010).

Baseline mixing section inlet conditions and reheat combustor operating conditions

The combustion properties of the NG-based and hydrogen-rich fuels were investigated with various hot-gas conditions at the inlet of the mixing section. Those conditions are the result of a certain HG operating condition and dilution air flow rate. A baseline mixing section inlet condition was defined as the standard for each fuel type, and is summarized in Table 2. Additional MS inlet conditions were investigated during the parameter studies and are described in subsequent sections.

Table 2: Baseline mixing section inlet conditions of NG (BL-NG) and hydrogen blends (BL-H_2)

		BL-NG	BL-H_2
p	[bar]	15	15
T_{MS}/ T_{BL-NG}	[-]	1	< 1
u	[m/s]	150	> u_{BL-NG}
x position fuel injection		FI_1	FI_2
d_{fi}	[mm]	2.4	5.6

In both cases, studies were carried out at an operating pressure of 15 bar and oxygen content of the hot gas entering the mixing section of around 15 vol. %. To account for the reduced ignition delay times and tightened flashback margin of H_2-rich fuels at elevated temperatures, the hot gas temperature in the MS (T_{MS}) at the baseline MS inlet condition of H_2 fuels (BL-H_2) was decreased by 100 K compared to that of the NG based fuels (BL-NG). For the same reason, the H_2-rich fuel was injected into the hot gas further downstream (at position FI_2) and at higher MS bulk velocities, which were increased by increasing the mass flow rates, leading to a shorter residence time of the reactive mixture in the MS. In addition, tests with NG + 25 vol. % propane (Wobbe Index 62 MJ/m^3 @ 273 K) were performed at the BL-NG MS inlet condition.

A carrier medium (N_2) was added to the fuel to achieve an adequate jet penetration depth. The carrier was perfectly premixed with the fuel to allow for mixing studies with planar laser-induced fluorescence (Tracer-PLIF) measurements planned in the future. The carrier-to-fuel mass flow ratio was 0.5 for the NG based fuels and 1 for the H_2/N_2 blend in order to adapt for the different momentum flux ratios (ratio of the jet to crossflow momentum), thereby achieving suitable penetration.

For the NG based fuels, which were injected at fuel/carrier temperatures of 303 - 323 K, the baseline operating condition in the reheat combustor corresponded to an equivalence ratio of the reheat combustor Φ_{reheat} of 0.5 and a thermal load of about 400 kW. For the H_2/N_2 blend, which had a fuel/carrier temperature of approximately 313 K, the set-point value was 80/20 vol. % (Wobbe Index 20 MJ/m^3 @ 273 K) at $\Phi_{reheat} = 0.4$. However, autoignition in the mixing section occurred at much lower H_2 concentrations, as will be discussed later.

Measuring techniques

The temperature in the mixing section (T_{MS}) was measured with a single thermocouple (TC-1) probe at the axis of symmetry (y = 0 mm) and held constant by a control loop. In addition, temperature profiles in the MS were measured at the two fuel injector positions, FI_1 and FI_2, at 5 vertical positions over the channel height in the centerline plane with a five-element thermocouple (TC-5) probe. Both probes are shielded with a ceramic casing to minimize radiative heat loss. The casing geometry is aerodynamically shaped to minimize flow field disturbances. The TC-1 probe is permanently installed in the upper MS wall, 60 mm upstream of position FI_1 and has a total length that is slightly longer than half of the channel height. The TC-5 probe can be mounted alternatively in either of the two fuel injector positions and spans almost the full channel height. It was only mounted during the temperature profile measurements, not during the optical and laser measurements.

Particle Image Velocimetry (PIV), with a set up described in (Fleck et al., 2010), was used to measure the velocity field in the MS centerline plane. The laser sheet (approximately 1 mm thick) was introduced into the MS from the top, while the signal was recorded with a Charge Coupled Device (CCD) camera from the side. The spatial resolution of the calculated velocity field was 3.2 mm (corresponding to an interrogation spot size of 32 x 32 pixels). TiO_2 particles with a nominal diameter of 1 µm were added to the dilution air, thereby seeding the hot gas in the mixing section.

The heat release in the flame root region of the reheat combustor was studied with OH* chemiluminescence measurements. The OH* chemiluminescence signal is emitted from electronically excited OH radicals (denoted OH*) with a very short lifetime that are formed in the heat release zone (Nori and Seitzman, 2007). Therefore, the detected signal is a good indicator of the line-of-sight integrated heat release zone. An image intensified CCD camera (LaVision Image Intense, 1376 x 1040 pixels) equipped with an achromatic UV lens (Halle, focal length = 65 mm) and a combination of a bandpass (295 - 320 nm) interference and UG 11 filter was used for signal detection. A series of 200 single shots, each with an exposure time of 40 µs, was recorded at each operating point.

Autoignition events were visualized with a high-speed camera (LaVision HSS6), which recorded the luminosity in the mixing section. A camera lens with a focal length of 85 mm and a focal ratio (f-number) of 1.4 was used. Images were recorded with a resolution of 1024 x 208 pixels at a recording rate of 20 kHz.

The integral gas composition and the emissions at the MS inlet were measured with an exhaust gas probe with 3 gas inlets, mounted horizontally at the MS inlet. A second single-hole probe mounted ≈ 80 mm downstream of the reheat combustor exit was used to measure the major species concentrations and pollutant emissions of the reheat combustor at the axis of symmetry. NO_x was measured via UV photometry (Limas 11), CO and CO_2 via IR photometry (Uras 14), and O_2 by paramagnetism (Magnos 16) at dry conditions. Unburned hydrocarbons (UHC) were measured with a flame ionization detector (Multi FID 14) at wet conditions.

RESULTS AND DISCUSSION

Mixing zone boundary conditions

The first objective was to investigate the hot gas composition, temperature homogeneity, and velocity field in the mixing zone of the reheat combustor. In order to achieve different temperatures at a hot gas composition of about 15 vol. % O_2, the hot gas generator (HG) must perform reliably over a broad operational range with

extremely low emissions. The HG emissions at the BL-NG MS inlet condition of p = 15 bar, a combustion air inlet temperature $T_{inlet, HG}$ = 793 K, and an equivalence ratio range of Φ_{HG} = 0.4 - 0.45 are shown in Figure 3. In general, extremely low emission levels were measured, with NO_x and CO in the single ppm range and no observed unburned hydrocarbons (UHC). As expected, the NO_x emissions strongly increased with increasing Φ_{HG}, from below 1 ppm at Φ_{HG} = 0.4 to slightly over 3 ppm at Φ_{HG} = 0.45. This can be explained by the exponential temperature dependence of thermal NO formation. Higher lean equivalence ratios result in higher temperatures and therefore increased NO formation. Very low CO concentrations below 2 ppm were measured. For BL-H_2 MS inlet conditions, not shown here, the emissions were at similar or even lower levels. Hence, the hot gas generator fully met the requirements of low emissions over a broad operational range. This allowed the variation of the MS inlet conditions by changing the HG operating conditions and the dilution air, without negative influences on emissions or flame stability.

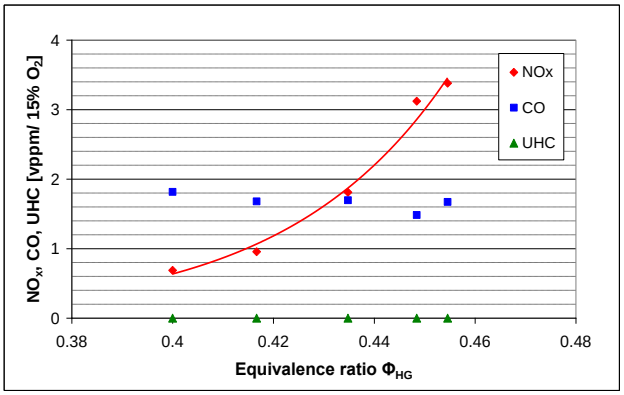

Figure 3: Hot gas generator emissions (NO_x, CO, UHC) for equivalence ratio variation; 15 bar, $T_{inlet,HG}$ = 793 K

The temperature in the mixing section (T_{MS1}) was measured with the permanently mounted TC-1 probe. The deviation of the measured mean T_{MS1} temperature from the design values was below 1% in all measurements, which is in the range of the relative standard deviation of T_{MS1} during the measurements and the day to day reproducibility. To verify the temperature homogeneity in the mixing section, temperature profiles at the two fuel injection positions, FI_1 and FI_2, were measured for different operating conditions. The temperatures measured at the axis of symmetry (y = 0 mm) at FI_1 or FI_2 were between 1 - 2% lower than T_{MS1} due to the small heat loss in the MS.

Figure 4 shows temperature profiles for two different design temperatures (T_{BL-NG}, T_{BL-NG} - 100 K) of the hot gas in the mixing section at a bulk velocity of 150 m/s and a pressure of 15 bar. In order to analyze the homogeneity of

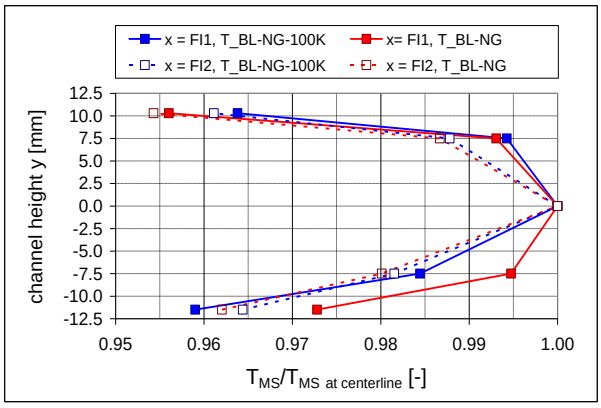

Figure 4: Normalized temperature profiles over the channel height measured for 2 mean hot gas temperatures (T_{BL-NG}, T_{BL-NG} - 100 K) at x positions FI_1 and FI_2, u = 150 m/s, 15 bar. Values are normalized by the T value at the axis of symmetry

the temperature profile, the values are normalized by their corresponding values at the axis of symmetry (y = 0 mm). In general, all profiles are symmetric and show a high temperature homogeneity in the middle of the channel (y = ± 7.5 mm), evidenced by a very small temperature decrease of less than 2%. The higher temperature gradient near the walls is caused by wall cooling effects. For a constant axial position, the measured temperature profiles at the two design temperature levels are very similar. However, the temperature profiles at FI_2 are steeper than those at FI_1 due to the higher overall heat loss at the more downstream position. This heat loss difference between the two x-positions was estimated to be about 1.5%.

The main flow velocity field in the MS was measured with PIV at the centerline plane for the two baseline MS inlet conditions BL-NG and BL-H_2. Since the results for both baselines exhibited similar characteristics with negligible vertical velocities, only the axial velocity field for BL-NG is presented in Figure 5. In general, the velocity distribution is quite uniform (colour scale is min-max). The wake of the TC-1 probe is apparent in the upper half of the mixing channel and causes a velocity deficit that decays with downstream distance. This results in an increase in the mean axial velocity in the centerline

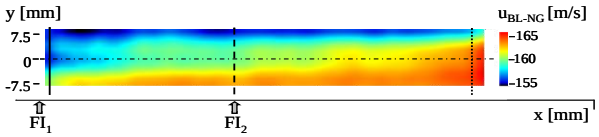

Figure 5: Axial velocity in the mixing zone without injected fuel at BL-NG MS inlet conditions.
Scaling: min-max

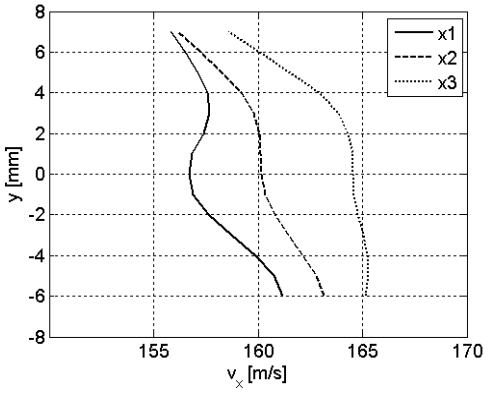

Figure 6: Axial velocity profiles at BL-NG MS inlet conditions at three different x positions (x_1: close to the upstream edge of the field of view, x_2: FI_2, x_3: close to the downstream edge of the field of view)

(measurement) plane in the axial direction. A second reason for the increased axial velocity is flow acceleration in the center region due to boundary layer growth in the axial direction. To investigate this in more detail, axial velocity profiles at three different x- positions are shown in Figure 6. The profiles show that the velocities in the upper half of the channel are about 3 - 4% lower than in the lower half. This indicates that the asymmetry is caused by the wake of the TC-1 probe mounted vertically in the upper half of the MS channel. The profile at x_1 shows a second small velocity deficit around the axis of symmetry, which might be a residue of a wake from the horizontally mounted emission probe at the MS inlet. The mean velocity at the three x-positions increased by about 4% from u = 158 m/s at the most upstream position to u = 164 m/s at the most downstream position. Furthermore, close to the MS exit (x_3), the averaged velocity measured with PIV exceeds the mass averaged value of 154 m/s (calculated with the hot gas mass flow rate, the hot gas density, and the MS cross-section of 25 x 25 mm without taking into account the boundary layer thickness), by about 11%. As stated earlier this is likely caused by the wall boundary layers, leading to a higher volumetric flow through the optically accessible centerline plane.

Natural gas (benchmark)

During the reheat combustor tests with natural gas injected at BL-NG MS inlet conditions, soft ignition and stable performance of the reheat combustor were observed at an equivalence ratio $\Phi_{reheat} = 0.5$. Within the optically accessible part of the reheat combustor, only a weak heat release zone could be detected with OH*-chemiluminescence. This indicates that a lifted flame was stabilized farther downstream, well detached from the cross-sectional jump.

The operating parameters were varied separately according Table 3. Relative to the baseline conditions (100%), the pressure was decreased to 33%, the MS inlet temperature increased by 100 K, the velocity decreased to 53%, the O_2 content was increased to 104%, and the Φ_{reheat} was increased to 125%.

Table 3: Parameter matrix

	mixing section				reheat comb.
	pressure	inlet temp.	velocity	O2-content	Phi_reheat
	p [bar]	T_in,MS [K]	u_in,MS [m/s]	O2_in, MS [Vol.%]	Φ
baseline NG:	100%	100%	100%	100%	100%
		+ 100 K	66%	104%	125%
			53%		
	33%				

In all NG tests, the reheat combustor operated stably, without any remarkable pressure pulsations, which were measured with fast (10 kHz) pressure transducers. Furthermore, no autoignition events occurred in the mixing section. Even at the most critical parameter set, with a 100 K higher temperature and a bulk velocity at the MS inlet reduced by a factor of two, no autoignition was observed.

In addition to the reheat combustor performance, the MS velocity field with injected fuel at BL-NG conditions was measured with PIV. For $\Phi_{reheat} = 0.5$, the fuel + carrier flow rate resulted in a momentum flux ratio of 7.5. Figure 7 shows averaged images of the axial (a), the vertical (b) and the rms velocity (c) measured in the centerline plane, with the rms values being the quadratic mean of the axial and vertical turbulent velocity fluctuations. Overall, the data exhibit the typical properties of a jet-in-crossflow configuration (Fric and Roshko, 1994; Yuan et al., 1999; Majander and Siikonen, 2006). The axial velocity plot shows that the crossflow was deflected and hence accelerated immediately upstream of the jet, leading to a low velocity region in the jet wake farther downstream.

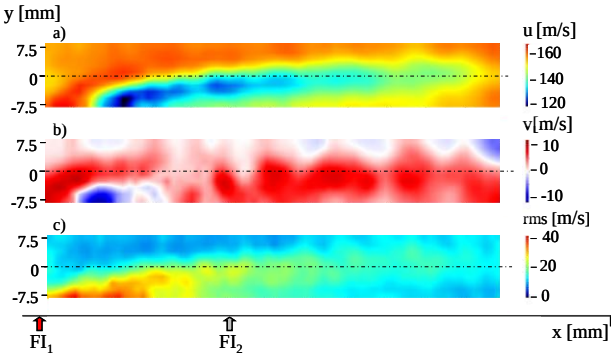

Figure 7: Averaged velocity field in the mixing section with NG injected at BL-NG conditions; a) axial velocity u, b) vertical velocity v, c) rms velocity. Scaling: min-max

The highest vertical velocities were measured at the most upstream edge of the field of view, close to the FI_1 position, and were caused by the vertical momentum of the penetrating jet. This region represents the shear induced vertical velocities of the seeded main flow mixed with the fuel jet. Since the fuel jet was not seeded, the jet core with its very high exit velocity (approx. 1.7 x u_{MS}) can not be seen. Directly downstream of this region, the negative vertical velocities indicate vortices in the jet wake. Even farther downstream, the positive vertical velocities in the region of the axis of symmetry indicate the existence of a counter rotating vortex pair (CVP), which decays much slower than the vorticity in the rest of the flow and becomes the dominant flow structure in the jet far field (Fric and Roshko, 1994; Yuan et al., 1999).

The region in which the rms velocities exceed the values of the main flow illustrates the upper boundary of the jet. This is due to high velocity gradients in the shear layer leading to enhanced turbulence production. The highest rms velocities are found in the wake directly behind the penetrating jet and are caused by the high vorticity in this region. In general, the velocity results show that the jet penetration was sufficient to reach the middle of the channel.

In Figure 8, two typical single shot images showing swirling strength (Adrian et al., 2000) are presented. Locations of high swirling strength indicate vortices in the jet shear layer. As in the averaged images, the vortex structures are more pronounced in the near field of the jet because in this region turbulence is generated due to shear. As a consequence of the turbulence cascade and viscous dissipation of the smallest turbulent scales, the swirling strength gets weaker as the vortices propagate downstream. The variation of the spot locations illustrates the shedding and motion of the vortices in the jet and the jet wake, which has already been observed e. g. in Yuan et al. (1999) and Rivero et al. (2001).

The reheat combustor tests with NG showed good and reliable performance, which is in agreement with the practical system. The absence of autoignition in the MS proves that the chosen fuel injection configuration, which leads to enhanced vorticity and hence higher residence times in the jet wake, did not increase the risk of autoignition with NG.

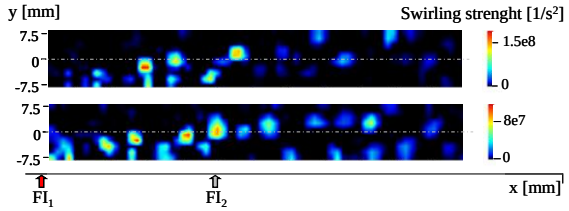

Figure 8: Instantaneous swirling strength in the mixing section with NG injected at BL-NG conditions. Scaling: 0-max

"Off-Spec" NG

In order to investigate the effects of NG with greater amounts of higher hydrocarbons ("off-spec" NG) on the reheat combustor performance, up to 25 vol. % propane was added to the NG. These measurements were performed at BL-NG conditions, keeping the equivalence ratio Φ_{reheat} constant at 0.5. With the constant equivalence ratio, increasing the propane content of the fuel by replacing NG led to a decreased momentum flux ratio, from J = 7.5 without propane to J = 5.5 with 25% propane, due to the higher fuel density and therefore lower jet velocity of the propane containing fuel. Figure 9 shows averaged OH* chemiluminescence images from the reheat combustor operated with fuels of increasing propane concentrations (0, 10, 20, 25 vol. %; a)-d)). For pure NG (image a), only a weak heat release zone could be detected since the flame was detached from the cross-sectional jump and located farther downstream of the optically accessible region. With higher propane concentrations, the flame stabilized closer to the cross-sectional jump, indicated by the larger and more intense region of OH* chemiluminescence signal. For NG with 25% propane (image d), part of the main heat release zone at the flame root is clearly visible. The heat release zone is slightly asymmetric, with the signal maximum in the lower channel half. This is partly related to the decreased momentum flux ratio with increasing propane concentration, which results in a slight under-penetration of the jet. The change in the flame position, with the flame moving closer to the cross-sectional jump with rising propane concentration, can be attributed to an increasing turbulent flame speed and a reduced ignition delay time with increasing propane concentration. This has been reported earlier by Boschek et

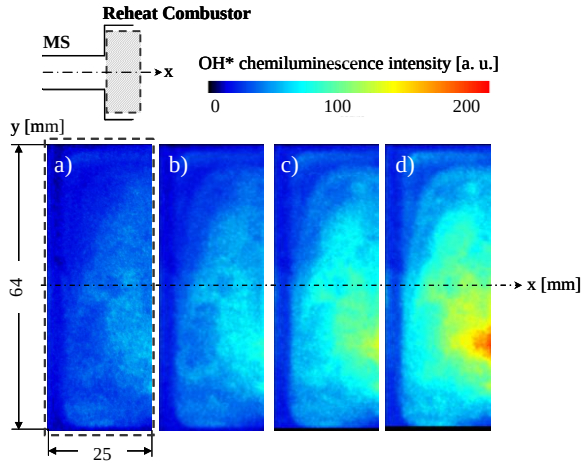

Figure 9: Averaged OH* chemiluminescence images of the reheat combustor operated with NG with different propane concentrations: a) 0, b) 10, c) 20, d) 25 vol. %

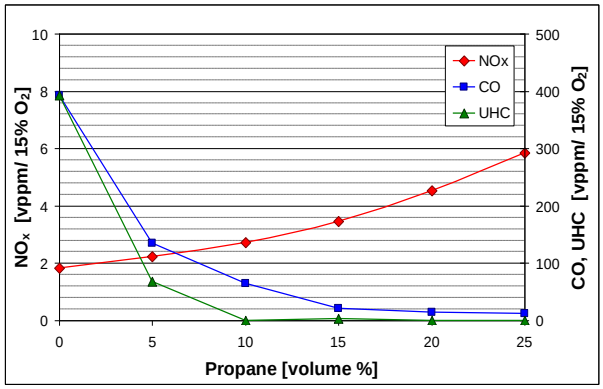

Figure 10: Emissions of the reheat combustor (NO_x, CO, UHC) operated with NG doped with different propane concentrations; MS inlet conditions: BL-NG

al. (2007).

The emissions of the reheat combustor are plotted versus the propane concentration in vol. % in Figure 10. For up to 10 vol. % propane, the measured UHC and CO concentrations are rather high, indicating that the residence time (a few ms) in the combustor is not sufficiently high to ensure complete combustion. When increasing the propane concentration to 25 vol. %, it can be observed that the UHC and CO concentrations strongly decrease and the NO_x concentration tripled. This behavior is a consequence of the changed flame position, leading to a change in the flow field and thereby to longer effective residence time in the combustor. This causes the UHC and CO to decrease and the NO_x to increase. In addition, the increase in NO_x is also partly due to an increase in the prompt NO formation pathway promoted by a higher CH_i radical concentration with a higher propane content, e.g. reported in Boschek et al. (2007).

No autoignition occurred in the mixing section during the "off-spec" NG tests. This is in line with the C_2^+ concentration limit of up to 16 vol. % for the technical system without any combustor hardware changes given in Riccius et al. (2005). This limit of course includes an additional safety margin and therefore is far from the occurrence of any flashback or autoignition.

H_2-rich fuel

Autoignition events with H_2 as a fuel were studied using a blend of H_2/N_2 at 80/20 vol. % (set-point value) and $\Phi_{reheat} = 0.4$. The mixture was injected at BL-H_2 MS inlet conditions together with a higher carrier medium flow rate (carrier-to-fuel mass flow ratio of CFR = 1). To adjust the fuel flow rate, the carrier and N_2 content of the fuel were first brought to their desired values, corresponding to the set-point value described above. The H_2 mass flow rate was then stepwise increased towards its set-point. At a H_2 mass flow rate corresponding to a fuel composition of around H_2/N_2 50/50 vol. % and J ≈ 1.3, autoignition in the mixing section occurred before the reheat combustor ignited. This procedure was repeated three times for the same operating condition, with autoignition events occurring at a similar fuel composition during every run. Since the autoignition occurred at transient operating conditions, the fuel composition at autoignition can only be determined with an accuracy of about ± 2%.

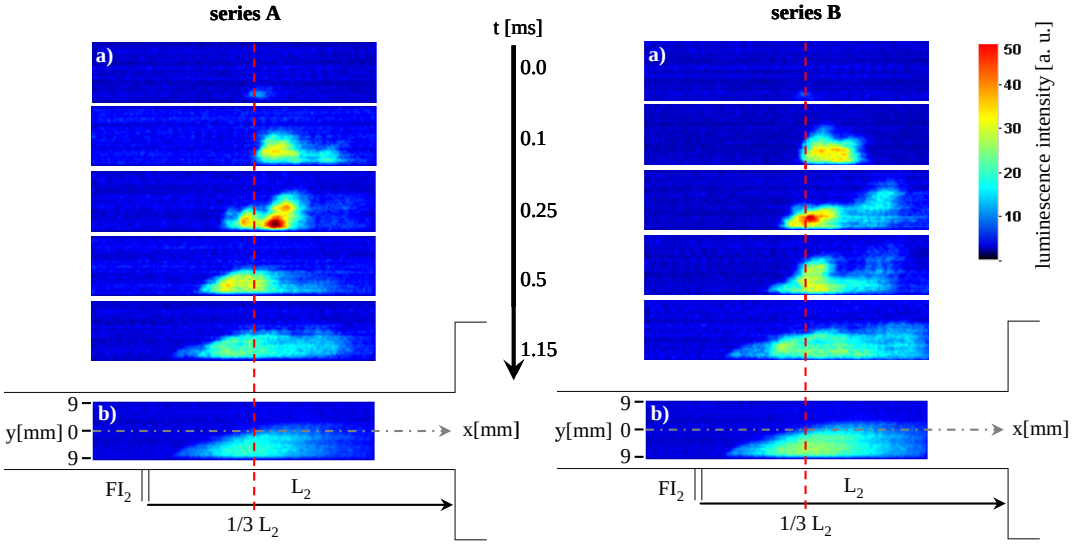

Figure 11: Series of high-speed images during two autoignition events (series A & series B) at corresponding nominal operating conditions of the reheat combustor (set-point H_2/N_2 80/20 vol. %), red line: initial autoignition kernel location; a) extracted single shot images; b) averaged images

Two of the three ignition events recorded with the high-speed camera (series A & series B) are presented in Figure 11. Figure 11a of each series describes the development of the autoignition event from a sequence of single shot high-speed images extracted from the whole series, with t = 0 ms being the time of the first occurrence of an autoignition kernel. In Figure 11b the luminosity images averaged over approximately 5000 frames after ignition of the main-jet are shown together with a sketch of the combustor geometry. For both series, the development of the ignition process in the mixing section is very similar. The first autoignition kernel occurs at an axial position (marked by the red vertical line) of about one third of the axial distance between fuel injection position FI_2 and the MS exit (L_2) and close to the lower wall. It increases in size and intensity, moving slightly in the downstream direction (2^{nd} image Fig. 11a) and then propagates upstream in the near wall region. The whole jet is ignited after about 1 ms (3^{rd} to 5^{th} image of Fig. 11a). It is very likely that the flame propagation happens in the boundary layer, the region with the lowest velocities. However, this region is not optically accessible due to design restrictions. The marginally higher intensity observed in the 5^{th} image and the average image of series B is due to the ignition occurring at a slightly higher H_2 concentration of about H_2/N_2 53/47 compared to approximately 46/54 in series A. This ≈15 % difference in the H_2 concentration at which the first autoignition kernel occurs is very likely related to the fact that autoignition is strongly effected by local temperature and stoichiometry conditions as well as by the specific time history of fluid parcels with respect to temperature, mixing and residence time. Hence, this difference might be attributed to small temperature fluctuations or velocity field fluctuations.

For further interpretation of these autoignition events, more detailed investigations including measurement of the mixing field must be performed. These measurements are planned for the future.

SUMMARY AND CONCLUSIONS

A geometrically scaled, optically accessible, generic reheat combustor has been developed to investigate fuel flexibility aspects, mainly with regard to autoignition at typical reheat conditions. Since the boundary conditions, namely temperature, velocity field, and gas composition, strongly influence autoignition, one focus of the present study was the careful characterization of the mixing section with respect to these parameters. In addition, the performance of the reheat combustor operating with natural gas as a benchmark as well as with a H_2/N_2 blend was investigated.

The results show that the design of the hot gas generator (HG) and mixing section (MS) fully met the requirements. The HG showed a broad operational range with good flame stability and extremely low emissions. Furthermore, temperature measurements at two fuel injection positions proved good temperature homogeneity, with a deviation in the middle of the channel of smaller than 2%. Velocity results measured with Particle Image Velocimetry showed a sufficiently smooth flow field.

Stable and quiet performance was observed when operating the reheat combustor with natural gas, with the flame root being detached from the cross-sectional jump. The velocity field measured with fuel injection exhibited the typical flow pattern of a jet-in-crossflow configuration. Even for the most critical parameter set in the MS and “off-spec” natural gas of up to 25 vol. % propane, no autoignition occurred in the mixing section. Partly replacing the NG with propane clearly changed the flame position and the reheat combustor emissions. The flame stabilized closer to the cross-sectional jump, reducing the CO and UHC emissions because of a higher residence time in the reheat combustor. However, the NO_x emissions increased for the same reason, together with a promoted prompt NO formation route due to higher CH_i radical concentration.

In contrast, when injecting a H_2/N_2 blend, autoignition in the MS occurred during ramping of the H_2 mass flow rate. The autoignition events were recorded with a high-speed camera at 20 kHz. The occurrence of autoignition for the present H_2/N_2 blend underlines the importance of investigating hydrogen containing fuels in context with reheat conditions.

The present study already documents interesting results with respect to fuel flexibility aspects that must be further investigated in a more detail. A mixing study planned for the future, e.g. will give additional information about the local stoichiometry and hence further elucidate the autoignition results.

ACKNOWLEDGMENTS

This work has been funded by ALSTOM® Power Generation AG, EnBW Holding AG and the “Ministerium für Wissenschaft, Forschung und Kunst (MWK) Baden-Württemberg” which is gratefully acknowledged. The authors would also like to thank U. Prestel, K. Ferst, S. Peukert, M. Kapernaum and D. Lebküchner for their technical support during the measurements.

REFERENCES

Adrian, R. J., Christensen, K. T., Liu, Z.-C., "Analysis and Interpretation of Instantaneous Turbulent Velocity Fields," Exp. Fluids, 29, 2000, pp. 275-290.

Boschek, E., Griebel, P. and Jansohn, P., "Fuel Variability Effects on Turbulent, Lean Premixed Flames at High Pressures," ASME, GT2007-27496, 2007, pp. 1-10.

Campbell, A., Goldmeer, J., Healy, T., Washam, R., Molière, M. and Citeno, J., "Heavy Duty Gas Turbines

Fuel Flexibility," ASME, GT2008-51368, 2008, pp. 1-9.

De Vries, J. and Petersen, E. L., "Autoignition of Methane-Based Fuel Blends under Gas Turbine Relevant Conditions," Proc. Combust. Inst., 31, 2007, pp. 3163-3171.

Fleck, J. M., Griebel, P., Steinberg, A. M., Stöhr, M., Aigner, M. and Ciani, A., "Experimental Investigation of a Generic, Fuel Flexible Reheat Combustor at Gas Turbine Relevant Operating Conditions," ASME, submitted, GT2010-22722, 2010, pp. 1-10.

Fric, T. F. and Roshko, A., "Vortical Structure in the Wake of a Transverse Jet," J. Fluid Mech., 279, 1994, pp. 1-47.

Güthe, F., Hellat, J., Flohr, P., "The Reheat Concept: The Proven Pathway to Ultralow Emissions and High Efficiency and Flexibility," J. Eng. Gas Turbines Power, 131, 2009, pp. 021503 1-7.

Herzler, J. and Naumann, C., "Shock-Tube Study of the Ignition of Methane/Ethane/Hydrogen Mixtures with Contents from 0% to 100% at Different Pressures," Proc. Combust. Inst., 32, 2009, pp. 213-220.

Huang, J. and Bushe, W. K., "Experimental and Kinetic Study of Autoignition in Methane/Ethane/Air and Methane/Propane/Air Mixtures under Engine-Relevant Conditions," Combust. Flame, 144, 2006, pp. 74-88.

Joos, F., Brunner, P., Schulte-Werning, B., Syed, K. and Eroglu, A., "Development of the Sequential Combustion System for the ABB GT24/GT26 Gas Turbine Family," ASME, 96-GT-315, 1996, pp. 1-11.

Koch, A., Naumann, C., Meier, W. and Aigner, M., "Experimental Study and Modeling of Autoignition of Natural Gas/Air-Mixtures under Gas Turbine Relevant Conditions," ASME, GT2005-68405, 2005, pp. 1-8.

Lechner C., Seume J., “Stationäre Gasturbinen,” Springer, Berlin Heidelberg, 2003.

Lee, U. D., Yoo, C. S., Chen, J. H. and Frank, J. H., "Effects of H_2O and NO on Extinction and Re-Ignition of Vortex-Perturbed Hydrogen Counterflow Flames," Proc. Combust. Inst., 32, 2009, pp. 1059-1066.

Lieuwen, T., McDonell, V., Petersen, E. and Santavicca, D., "Fuel Flexibility Influences on Premixed Combustor Blowout, Flashback, Autoignition, and Stability," J. Eng. Gas Turbines Power, 130, 2008, pp. 011506 1-10.

Lückerath, R., Meier, W. and Aigner, M., "FLOX® Combustion at High Pressure with Different Fuel Compositions," J. Eng. Gas Turbines Power, 130, 2008, pp. 011505 1-7.

Majander, P. and Siikonen, T., "Large-Eddy Simulation of a Round Jet in a Cross-Flow," Int. J. Heat and Fluid Flow, 27, 2006, pp. 402-415.

Mittal, G., Sung, C. and Yetter, R. A., "Autoignition of H_2/CO at Elevated Pressures in a Rapid Compression Machine," Int. J. Chem. Kinet., 38, 2006, pp. 516-529.

Nori, V. N. and Seitzman, J. M., "Chemiluminescence Measurements and Modeling in Syngas, Methane and Jet-A Fueled Combustors," AIAA paper, AIAA-2007-466, 2007, pp. 1-14.

Petersen, E. L., Hall, J. M., Smith, S. D. and de Vries, J., "Ignition of Lean Methane-Based Fuel Blends at Gas Turbine Pressures," J. Eng. Gas Turbines Power, 129, 2007, pp. 937-944.

Riccius, O., Smith, R., Güthe, F. and Flohr, P., "The GT24/26 Combustion Technology and High Hydrocarbon ("C2+") Fuels," ASME, GT2005-68799, 2005, pp. 1-8.

Rivero, A., Ferré, J. A. and Giralt, F., "Organized Motions in a Jet in Crossflow," J. Fluid Mech., 444, 2001, pp. 117-149.

Yuan, L. L., Street, R. L. and Ferziger, J. H., "Large-Eddy Simulations of a Round Jet in Crossflow," J. Fluid Mech., 379, 1999, pp. 71-104